

# Electronic and optical properties of GaS: A first-principles study

Bahattin ERDINC<sup>1\*</sup>, Harun AKKUS<sup>1</sup>, Kadir GOKSEN<sup>1</sup>

<sup>1</sup>*Yuzuncu Yil University, Physics Department, 65080, Van, Turkey*

*Received: 05.04.2010 Revised: 02.05.2010 Accepted: 12.05.2010*

---

## ABSTRACT

The electronic band structure and optical properties of hexagonal GaS are investigated using the density functional theory. The calculated band structure shows that the crystal has an indirect band gap with the value of 1.54 eV in the Brillouin zone at the  $\Gamma \rightarrow M$ . The structural optimization has been performed using the generalized gradient approximation (GGA) and the local density approximation (LDA). The calculated structure optimization of GaS has been compared with the experimental results and has been found to be in good agreement with each other. Furthermore, the linear photon-energy-dependent dielectric functions and some optical constants such as energy-loss functions for volume and surface, extinction, reflectivity and absorption coefficients, refractive index and effective number of valence electrons per unit cell participating in the interband transitions have been calculated.

**Key Words:** *Density functional theory, local density approximation, gradient and other corrections; Optical properties; Electronic structure; Optical constants.*

---

## 1. INTRODUCTION

In recent years, several binary and ternary layered semiconductors have attracted a lot of interest due to their future optoelectronic applications in ultraviolet, visible and infrared regions of the spectra [1, 2]. Since these materials have large optical nonlinearity, they are also promising for optical switching devices. Besides, they

can be used as photoelectric analyzers of polarized light, too [3]. Despite the significant number of experimental and theoretical studies on these materials, it is seen that neither the experimental data nor the overall theoretical understanding of them are sufficient to be qualified as a complete and coherent framework. Actually, only a little

---

\*Corresponding author, e-mail: bahattinerdinc@yyu.edu.tr

work has been done both experimentally and theoretically even for binary compounds, like GaS.

GaS is a member of the family of the  $A^{III}B^{VI}$  type semiconductor crystals, crystallizing in a layered structure, like GaSe and InSe. These layered compounds are characterized by highly anisotropic bonding forces arising from the fact that layer-layer interaction is weaker than the bonding force within a layer. In GaS, intralayer-bonding forces are ionic covalent type, whereas interlayer ones are van der Waals type, which causes a weak interlayer interaction between layers. Due to this property, GaS can easily be cleaved along these layers. GaS crystallizes in the so-called  $\beta$ -polytype and carries the symmetry properties of the  $P6_3/mmc$  (No. 194) space group. Each layer consists of four atoms stacked along the  $c$ -axis with a repeating unit of S–Ga–Ga–S and a unit cell has two layers, that is, eight atoms.

GaS has wide indirect and direct band gaps having the energy values of 2.59 and 3.04 eV at 300 K, respectively [4]. Due to the energy value of its band gap, this crystal is a promising material, especially for near-blue light emitting devices. The lattice vibrations in GaS crystal have been studied by several authors using Raman scattering [5-11], infrared reflectivity and absorption [12], inelastic neutron scattering [13], and Brillouin scattering measurements [14]. In addition to these, the trapping parameters have been investigated by thermally stimulated current measurements [15]. Furthermore, it has been experimentally revealed that GaS exhibits both electroluminescence and photoluminescence in the green-blue region [16-18]. Near band edge photoluminescence spectra of Zn doped and undoped GaS crystal has been investigated by various authors [19-21]. Besides, deep level luminescence was also observed experimentally for GaS crystal [22]. Moreover, a detailed low temperature photoluminescence study on GaS crystal has been reported, where the emission bands were thought to originate from close donor–acceptor pair recombination processes by using the results of excitation light intensity and temperature-dependent measurements [23, 24].

The present study focuses on the electronic and optical properties of GaS crystal using density functional theory under the local density approximation (LDA) and generalized gradient approximation (GGA) absent in the literature.

## 2. COMPUTATIONAL DETAILS

The self-consistent norm-conserving pseudopotentials were generated by using the FHI98PP code [25] with a Troullier-Martins scheme [26] for all atoms of GaS crystal. The Perdew-Burke-Ernzerhof GGA functional (PBE-GGA-96) [27] and Ceperley-Alder-Perdew-Wang LDA functional (CAPW-LDA-92)[28] were used to include the exchange-correlation effects. The pseudopotentials for only valence electrons were generated to investigate the effects on the physical properties of the crystal. 4s and 3p electrons of a Ga atom and 3s and 3p electrons of an S atom were studied as the true valence. The basis set for the electronic wave functions were chosen to be plane waves. The conjugate gradient minimization method [29] was used with the ABINIT code [30] for solving Kohn-Sham equations [31]. All the calculations included hexagonal unit cells containing four molecules. With the choice of cut-off energies at 35 hartree using  $8 \times 8 \times 8$  Monkhorst-

Pack mesh grid [32], a good convergence for the bulk total energy calculation was succeeded. On the other hand, the irreducible Brillouin zone was sampled with  $10 \times 10 \times 10$  k-points to calculate the optical properties of GaS.

For a material having a polar crystal structure and a spontaneous polarization,  $\vec{P}_s$ , the total polarization consists of two terms:  $\vec{P}_{tot} = \vec{P}_s + \vec{P}_i$ , where  $\vec{P}_i$  is the polarization induced by incoming light and given by formula [33]

$$P^i(\omega) = \chi_{ij}^{(1)}(-\omega, \omega)E^j(\omega) + \chi_{ijk}^{(2)}E^j(\omega)E^k(\omega) + \dots \quad (1)$$

In Eq. (1),  $\chi_{ij}^{(1)}$  is the frequency-dependent linear optical susceptibility tensor and is given by

$$\begin{aligned} \chi_{ij}^{(1)}(-\omega, \omega) &= \frac{e^2}{\hbar\Omega} \sum_{nm\vec{k}} f_{nm}(\vec{k}) \frac{r_{nm}^i(\vec{k})r_{mn}^j(\vec{k})}{\omega_{mn}(\vec{k}) - \omega} \\ &= \frac{\varepsilon_{ij}(\omega) - \delta_{ij}}{4\pi} \end{aligned} \quad (2)$$

where  $n$ ,  $m$  denote energy bands,  $f_{mn}(\vec{k}) \equiv f_m(\vec{k}) - f_n(\vec{k})$  is the Fermi occupation factor,  $\Omega$  is the volume,  $\omega_{mn}(\vec{k}) \equiv \omega_m(\vec{k}) - \omega_n(\vec{k})$  is the frequency differences,  $\hbar\omega_n(\vec{k})$  is the energy of band  $n$  at wave vector  $\vec{k}$ ,  $\varepsilon_{ij}(\omega)$  is the frequency-dependent dielectric tensor, and the  $r_{nm}$  are the matrix elements of the position operator. It is seen from Eq. (2) that the dielectric function can be associated with the susceptibility:  $\varepsilon_{ij}(\omega) = 1 + 4\pi\chi_{ij}^{(1)}(-\omega, \omega)$ . In Eq.

(1)  $\chi_{ijk}^{(2)}$  is the frequency-dependent second-order susceptibility tensor, but non-linear optical response for hexagonal GaS single crystal has not been investigated in this work.

It is a well-known fact that the properties of ground-state are determined by Kohn-Sham equations. The self-energy effects must be included when the optical response calculations are made, since the unoccupied conduction bands have no physical importance and a band gap problem appears at too low energy values. In order to include the self-energy effects, the scissor approximation [34] was used and 1.05 eV was chosen as the scissor shift in the present work using the experimental energy gap (2.59 eV) for GaS by Aulich *et al.* [4].

## 3 RESULTS AND DISCUSSION

### 3.1. Volume Optimization

The GaS crystal is hexagonal and belongs to the space group  $P6_3/mmc$  (No. 194). The investigated GaS contains two molecules with eight atoms per unit cell, as shown in Table 1. Calculations were carried out using the lattice constant  $a = b = 3.592 \text{ \AA}$  and  $c = 15.465 \text{ \AA}$  for GaS. The crystal data of GaS obtained the structure optimization from first-principle are presented in Table 2.

Table 1. Crystal structure data of hexagonal GaS.

Space group	P6 <sub>3</sub> /mmc					
GaS	Experimental [4]	Atom	Wyckoff	x	y	z
<i>a</i> (Å)	3.592	Ga	4f	0.3333	0.6667	0.17082
<i>c</i> (Å)	15.465	S	4f	0.3333	0.6667	0.60191
E <sub>g</sub> (eV)	2.59					
Volume (Å <sup>3</sup> )	172.8					

Table 2. Crystal structure data of hexagonal GaS from first-principle.

Space group	P6 <sub>3</sub> /mmc						
GaS	Calculated		Atom	Wyckoff	x	y	z
	GGA	LDA					
<i>a</i> (Å)	3.6406	3.4629	Ga	4f	0.3333	0.6667	0.17279
<i>c</i> (Å)	15.5137	15.3359	S	4f	0.3333	0.6667	0.60330
E <sub>g</sub> (eV)	1.54	1.54					
Volume (Å <sup>3</sup> )	178.1	159.3					

All physical properties of a material are related to the total energy. For example, the equilibrium lattice constant of a crystal is the lattice constant that minimizes the total energy. Therefore, physical properties of a material can be determined by the calculation of the total energy. In theoretical lattice constant calculations, the base state

energy of GaS crystal is calculated for different volumes around the experiment balance volume. Figure 1 shows the total energy as a function of the volume of GaS by the GGA and the LDA. The experimental and calculated volume values are presented in tables 1 and 2, respectively.

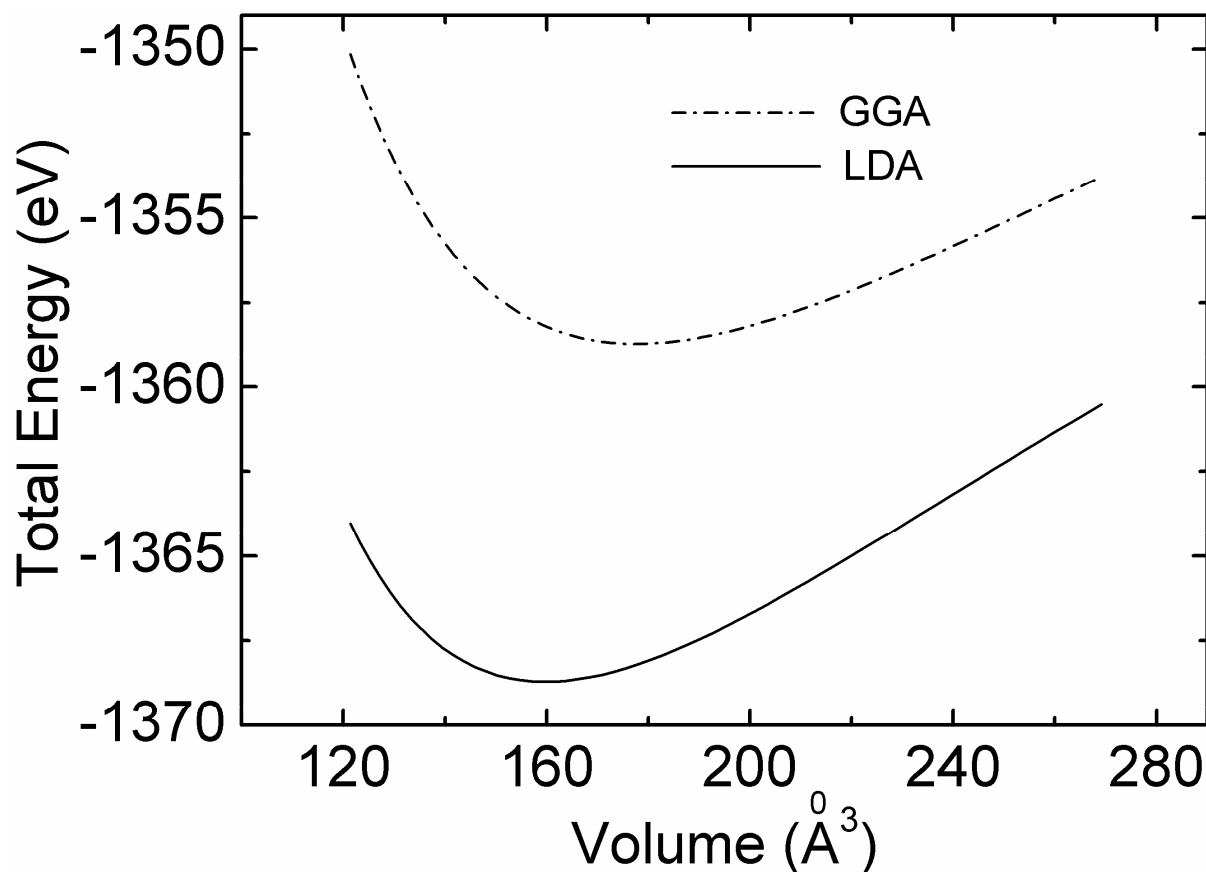


Figure 1. Dependence of total energy on unit cell volume for hexagonal GaS single crystal.

The lattice parameter of GaS can also be obtained using the pseudopotential method based on the density functional theory under the LDA and the GGA, that is, by minimization of the crystal total energy to crystal volume ratio (volume optimization), the theoretical lattice constants have been obtained as  $a = b = 3.4629 \text{ \AA}$  and  $c = 15.3359 \text{ \AA}$ ,  $a = b = 3.6406 \text{ \AA}$  and  $c = 15.5137 \text{ \AA}$ , respectively. The experimental and calculated data from first principles for the equilibrium lattice are given in tables 1 and 2.

The results reveal that the calculated values for the GGA are much closer to the experimental data than the calculated values for the LDA, which means that there are noticeable differences between the experimental data and the calculated data from LDA. As can be seen from

table 2, the deviation of the calculated equilibrium volumes for the GGA and the LDA calculations are 3.07% and 7.81% of the experimentally determined value, respectively. However, geometrical optimization using the LDA is more acceptable than that using the GGA, as shown in figure 1.

### 3.2. Band Structure and Density of States

The investigation of electronic band structure of hexagonal GaS is very useful for that it helps us to understand the electronic and optical properties of the material better. At this point, what we first need is to describe our calculated electronic structure. The energy-band structure calculated using the GGA for hexagonal GaS is shown in figure 2, where the origin of energy was arbitrarily set to be at the valence band maximum.

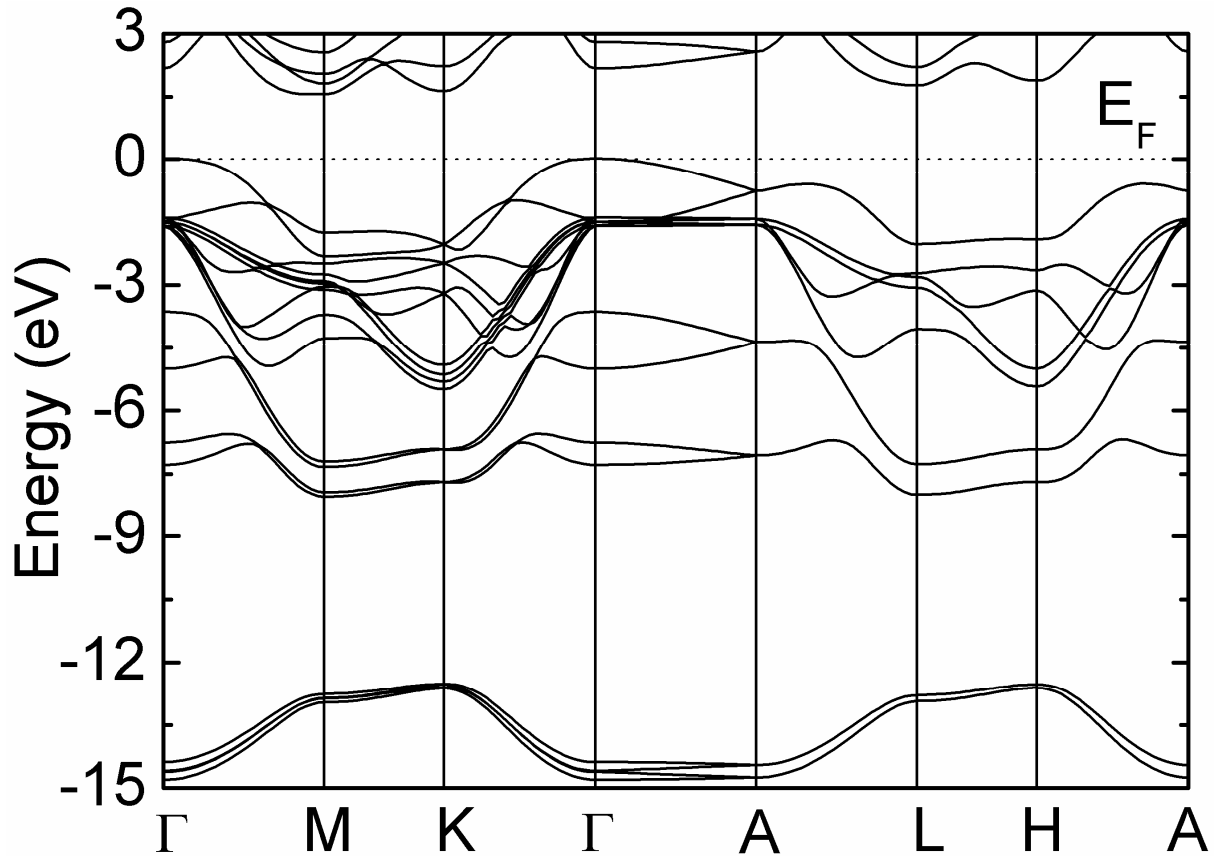


Figure 2. Calculated band structure for hexagonal GaS single crystal.

The band structure calculations have been performed in the high-symmetry directions of the first BZ. The band structure of hexagonal GaS has been calculated and plotted on surface of the BZ. The  $k$  points denoting the high symmetry points of irreducible BZ are marked with letters in figure 2, where the Fermi level is set to zero. The maximum of the valence band and minimum of the conduction band are located at the  $\Gamma \rightarrow M$  point of the BZ.

The calculated band structure for hexagonal GaS shows an indirect band gap at the  $\Gamma \rightarrow M$  symmetry direction of the BZ. The band gap

calculated by the GGA is 1.54 eV at the  $\Gamma \rightarrow M$  point. It is seen that the obtained band gap is smaller than the experimental result of 2.59 eV [4], probably due to a discrepancy in the pseudopotential method. If we add a correction factor to this band gap, the result is found to be in good agreement with the experimental result. Furthermore, total density of states (DOS) for GaS is also studied and the calculated DOS are shown in figure 3.

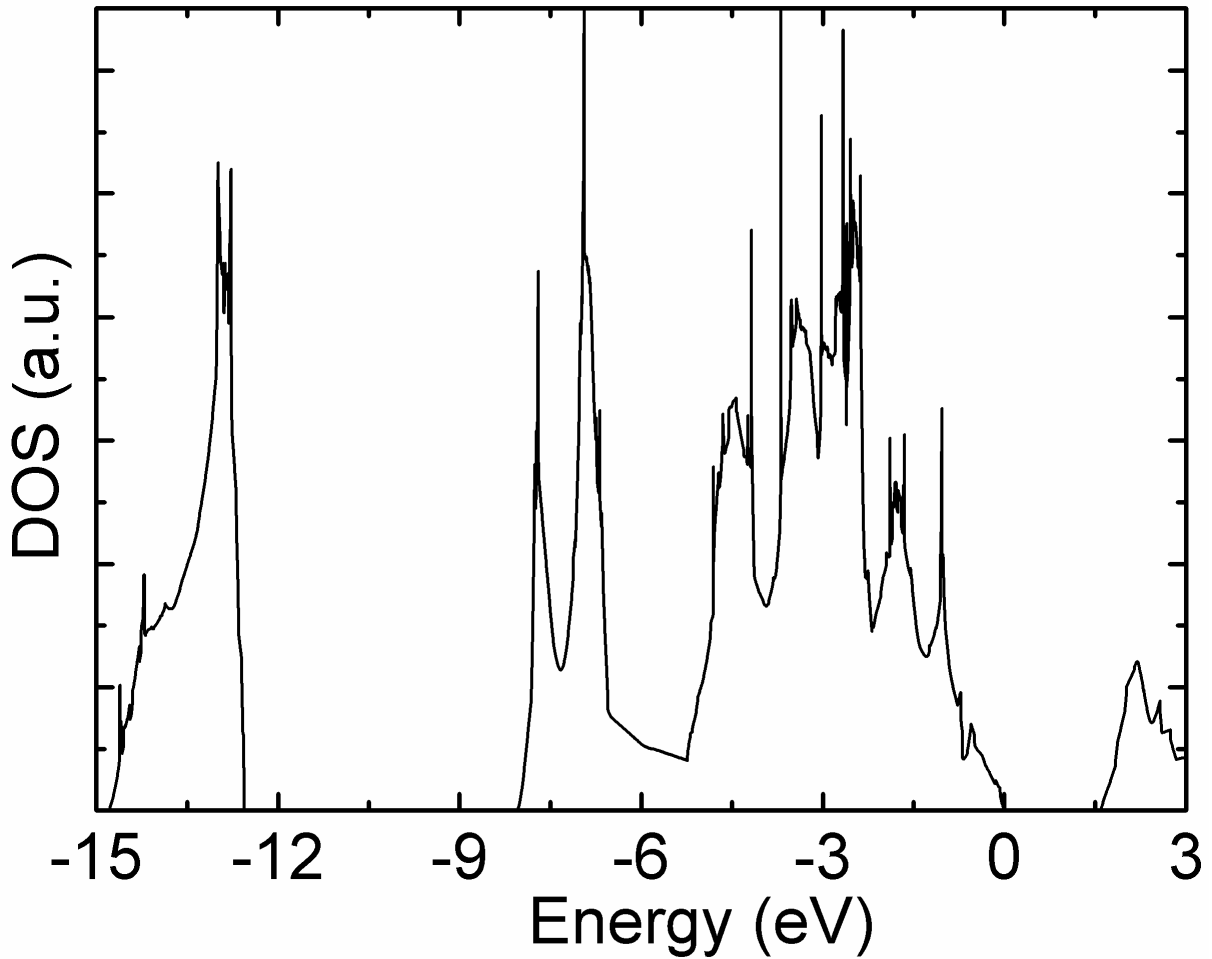


Figure 3. Total density of states for hexagonal GaS single crystal.

### 3.3. Optical Properties

In the present work, we also studied the linear optical properties of hexagonal GaS. The optical functions calculated by neglecting all lattice vibrational effects and pertaining only the electronic transitions are shown in figure 4. The optical response was calculated in the photon energy range of 0-30 eV by using the calculated band structure. As a result of calculations, we saw that a 0-25 eV photon-energy range is sufficient for most optical functions. Thus, we have derived the values of real and imaginary parts of the dielectric function as a function of the photon energy.

The calculated real and imaginary parts of the frequency-dependent linear dielectric function are shown in figure 4a and 4b along crystallographic *a*- and *c*-directions, respectively. Along the crystallographic *a*-direction, the imaginary part of the dielectric constant,  $\mathcal{E}_2$ , shows several main peaks located at 4.30, 5.0, 6.52, 6.95, 7.79, 8.48, 9.06, 10.39 and 11.26 eV, while along the crystallographic *c*-direction, it reveals peaks located at 3.95, 5.01, 5.48, 6.70, 7.79, 8.60, 9.15, 11.26, 11.78 and 12.76 eV. These peaks correspond to the optical transitions from the valence band to the conduction band. In the light of this information, we see that GaS exhibits two fundamental oscillator bands at 4.30 and 5.0 eV along crystallographic *a*- and another two fundamental oscillator

bands at 3.95 and 5.0 eV along crystallographic *c*-directions, respectively. From figure 4a, it is seen that 0-4.5 eV photon-energy range is characterized by high transparency, no absorption and a small reflectivity which explain the origin of the peak structure in the reflectivity and absorption coefficient spectra. In addition, 4.5-6.50 eV photon-energy range is characterized by strong absorption and appreciable reflectivity which means that optical absorption increases more quickly in this photon-energy range. Moreover, 6.50-11.50 eV photon-energy range is characterized by high reflectivity. Similarly, it is obvious from figure 4b that 0-3.95 eV photon-energy range is characterized by high transparency, no absorption and a small reflectivity, which explain the origin of the peak structure in the reflectivity and absorption coefficient spectra. Besides, the 3.95-5.48 eV photon-energy range is characterized by strong absorption and appreciable reflectivity, which means that optical absorption increases more quickly in this photon-energy range. Furthermore, 5.48-12 eV photon-energy range is characterized by high reflectivity.

Figure 4a and 4b also show the real parts of the frequency-dependent linear dielectric functions obtained from the imaginary parts by Kramers-Kronig conversion for crystallographic *a*- and *c*-directions, respectively. The static dielectric constants  $\epsilon_0$  of GaS is calculated as 5.56 along *a*-direction, while calculated as 7.26 along *c*-

direction. The function  $\mathcal{E}_1$  is equal to zero at 7.04, 8.18, 8.31 and 16.06 eV for *a*-direction and at 7.73, 8.31 and 18.08 eV for *c*-direction. The interband transitions at these points consisting mostly of plasmon excitations, the scattering probability of volume and surface losses are directly connected to the energy loss function.

For GaS, the calculated energy-loss functions,  $-Im \epsilon^{-1}$  for volume and  $-Im (1+\epsilon)^{-1}$  for surface, are plotted in figures 4c and 4d corresponding to crystallographic *a* and *c*-directions, respectively. The energy-loss functions give a description about the energy loss of the fast electrons transferring the material. The calculated energy-loss function for volume shows mainly two intense maximum peaks at 16.06 along *a*- and 18.43 eV along *c*-direction due to the excitation of plasmons. Furthermore, the calculated energy-loss function for surface shows mainly two intense maximum peaks at 13.50 and 14.75 eV, along *a*- and *c*-directions, respectively. It is easily noticed that the peak values of volume loss coincide with one of the zero values of the real part of dielectric function. The sharp maxima in the energy-loss functions are associated with the existence of plasma oscillations or the energy  $\hbar\omega_p$  of volume and surface plasmons. The calculated extinction coefficients, reflectivity spectrum, absorption coefficients and effective number of valence electrons along the crystallographic *a* and *c*-directions are shown in figures 4e, 4f, 4g and 4h, respectively.

The sum rule [35] can be used to calculate the effective number of valence electrons per unit cell contributing to the optical constants in the interband transitions. For both intraband and interband transitions, an estimate of the

distribution of oscillator strengths can be obtained by computing the  $N_{eff}(E_0)$  defined according to

$$N_{eff}(E_0) = \frac{2m\epsilon_0}{\pi\hbar^2 e^2} \frac{1}{N_0} \int_0^{E_0} \epsilon_2(E) E dE, \quad (2)$$

where  $N_{eff}(E_0)$  is the effective number of electrons contributing to optical transitions below an energy of  $E_0$ .  $E_0$  denotes the upper limit of integration, the quantities  $m$  and  $e$  are the electron mass and charge, respectively, and  $N_0$  stands for the electron density. As can be seen from figure 4h, the effective electron number,  $N_{eff}(E_0)$  along the crystallographic *a* and *c*-directions, up to 4.0 eV is zero, then rises rapidly and reaches a saturation value above 14.0 and 15.0 eV, respectively. This shows that the interband transitions do not include deep-lying valence states.

For the calculation of the refractive index, an initial choice of photon-wavelength range of 0-3  $\mu\text{m}$  was made. It was noticed that a 0-3  $\mu\text{m}$  photon-wavelength range is sufficient for the calculations, as seen from figure 5. The figure represents spectral dependence of the calculated main refractive index for hexagonal GaS in a wide wavelength range and reveals the decreasing behavior of  $n$  with the transition from the intrinsic absorption region towards long wavelengths where a normal dispersion takes place. In the figure, by using  $n = n(\lambda)$  dependence, the maxima are obtained at  $\lambda = 0.198$  and  $0.254 \mu\text{m}$  with the values of  $n$  as 3.694 and 4.074, along the crystallographic *a* and *c*-directions, respectively.

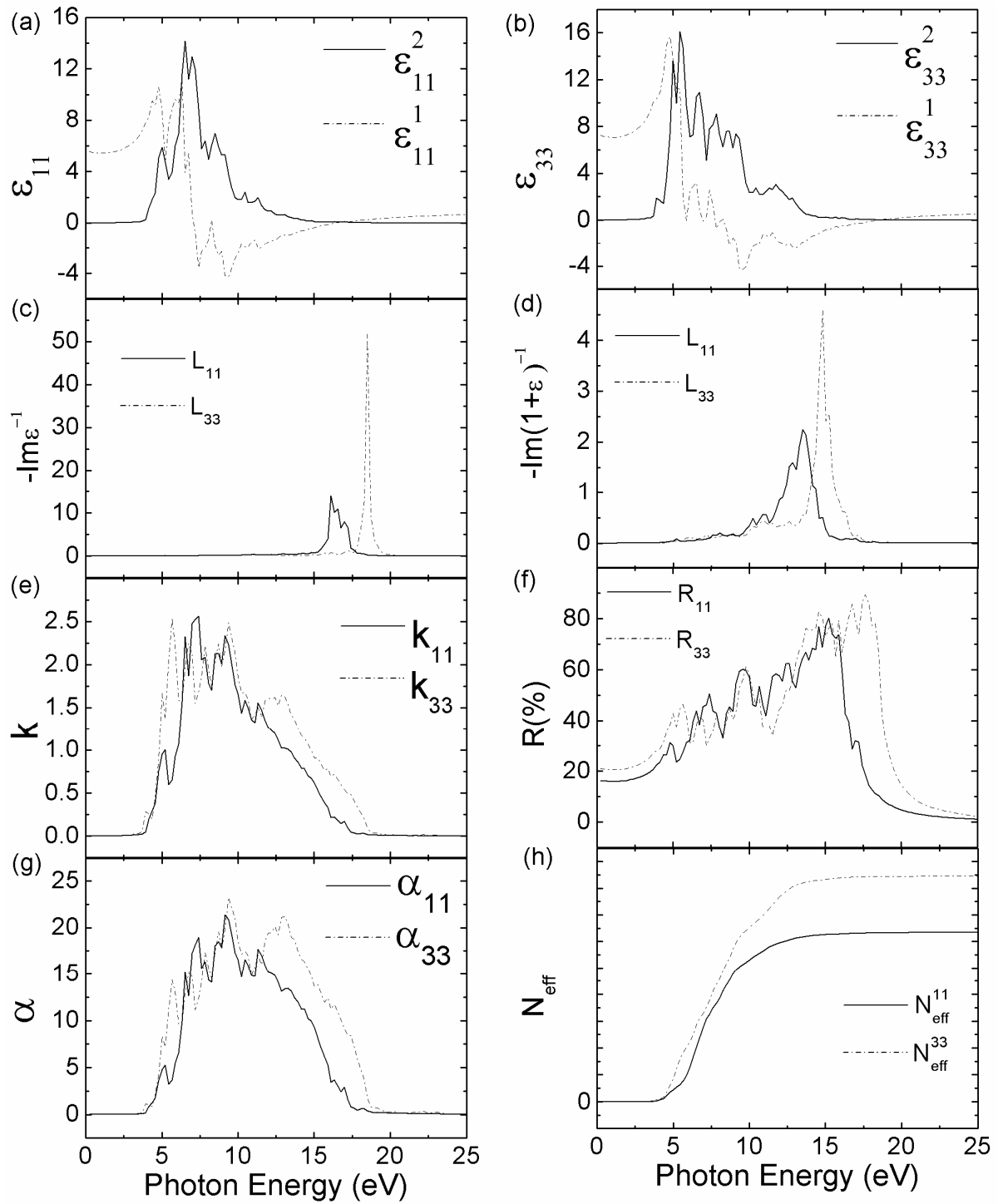


Figure 4. Optical spectra of hexagonal GaS crystal. Calculated real and imaginary parts of optical dielectric function, energy loss functions for volume and surface, extinction coefficient, reflectivity spectrum, absorption coefficient and effective number of valence electrons.



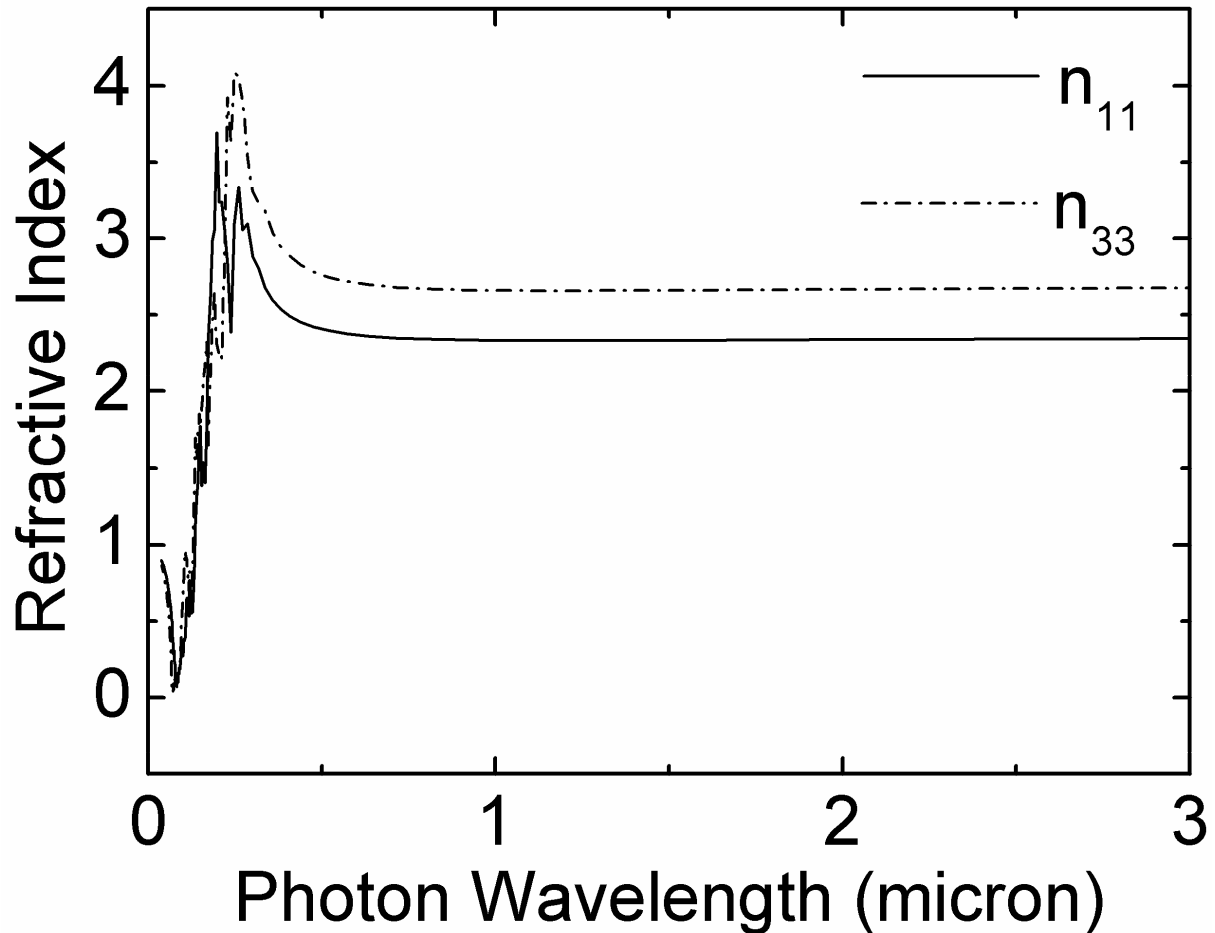


Figure 5. Dispersion of refractive index for hexagonal GaS crystal.

#### 4. CONCLUSIONS

In the present work, the electronic and linear optical properties of hexagonal GaS crystal have been investigated in detail by using the density functional methods under the GGA and LDA. As a result of calculations, it is found that the fundamental gap of GaS crystal is indirect at the  $\Gamma \rightarrow M$  point of the BZ. The calculated band gap by LDA is 1.54 eV at the  $\Gamma \rightarrow M$  points and is smaller than the experimental result of 2.59 eV because of the discontinuity in the pseudopotential method. We have examined the photon energy-dependent dielectric functions as well as related quantities such as energy-loss functions for volume and surface, extinction and absorption coefficients, reflectivity and refractive index. In addition to these, the effective number of valence electrons per unit cell participating in the interband transitions, which is a very important optical parameter, was studied and calculated. The results of implemented structural optimization by the GGA and LDA and the experiments agree with each other well.

#### ACKNOWLEDGMENTS

This research was supported in part by TUBITAK through TR-Grid e-Infrastructure Project and Yuzuncu Yil University under 2008-FED-B080 Project Number.

#### REFERENCES

- [1] Yee, K.A., Albright, A., "Bonding and structure of gallium thallium selenide ( $\text{GaTlSe}_2$ )", *J. Am. Chem. Soc.*, 113: 6474-6478 (1991).
- [2] Kyazym-zade, A.G., Mekhtieva, R.N., Akhmedov A.A., *Sov. Phys. Semicond.*, 25: 840 (1992).
- [3] Mekhtiev, N.M., Rud, Yu V., Salaev, E., Yu., *Sov. Phys. Semicond.*, 12: 924 (1978).
- [4] Aulich, E., Brebner, J.L., Mooser, E., "Indirect Energy Gap in GaSe and GaS", *Phys. Status Solid*, 31: 129-131 (1969).
- [5] Irwin, J.C., Hoff, R.M., Clayman, B.P., Bromley, R.A., "Long wavelength lattice vibrations in GaS and GaSe", *Solid State Commun.*, 13: 1531-1536 (1973).
- [6] Lucazeau, G., "Vibrational spectra of a GaS single crystal", *Solid State Commun.*, 18: 917-922 (1976).
- [7] Gasanly, N.M., "Effect of Crystal Disorder on Line Width Broadening of Phonon Modes in  $\text{GaS}_{1-x}\text{Se}_x$  Layered Mixed Crystals", *Crystal Research and Technology*, 38: 962-967 (2003).
- [8] Gasanly, N.M., Goncharov, A.F., Melnik, N.N., Ragimov, A.S., "Optical Phonons in  $\text{GaS}_{1-x}\text{Se}_x$

- Layer Mixed Crystals”, *Phys. Stat. Sol. (b)*, 120: 137-147 (1983).
- [9] Gasanly, N.M., Aydinli, A., Ozkan, H., Kocabas, C., “Temperature Dependence of the First-order Raman Scattering in GaS Layered Crystals”, *Solid State Commun.*, 116: 147-151 (2000).
- [10] Gasanly, N.M., Aydinli, A., “Low-temperature Raman Scattering Spectra of Ga<sub>1-x</sub>Se<sub>x</sub> Layered Mixed Crystals”, *Crystal Res. Technol.*, 37: 1011-1017 (2002).
- [11] Gasanly, N.M., “Compositional dependence of the Raman line shapes in GaS<sub>x</sub>Se<sub>1-x</sub> layered mixed crystals”, *J. Raman Spectroscopy*, 36: 879-883 (2005).
- [12] Riede, V., Neumann, H., Nguyen, H. X., Sobotta, H., Levy, F., “Polarization-dependent infrared optical properties of GaS”, *Physica B*, 100: 355-363 (1980).
- [13] Powell, B.M., Jandl, S., Brebner, J.L., Levy, F., “Anisotropic phonon dispersion in GaS”, *J. Phys. C: Solid State Phys.*, 10: 3039 (1977).
- [14] Polian, A., Besson, J.M., Grimsditch, M., Vogt, H., “Elastic properties of GaS under high pressure by Brillouin scattering”, *Phys. Rev. B*, 25: 2767-2775 (1982).
- [15] Gasanly, N.M., Aydinli, A., Yuksek, N.S., Salihoglu, O., “Trapping Centers in Undoped GaS Layered Single Crystals”, *Applied Physics A - Materials Science and Processing*, 77: 603-606 (2003).
- [16] Akhundov, G., Aksyanov, I.G., Gasumov, G.M., *Sov. Phys. Semicond.*, 3: 767 (1969).
- [17] Karaman, M.I., Mushinskii, V.P., *Sov. Phys. Semicond.*, 4: 662 (1970).
- [18] Cingolani, A., Minafra, A., Tantalo, P., Paorici, C., “Edge emission in GaSe and GaS”, *Phys. Status Solidi A*, 4: K83-K85 (1971).
- [19] Aono, T., Kase, K., Kinoshita, A., “Near-blue photoluminescence of Zn-doped GaS single crystals”, *J. Appl. Phys.*, 74: 2818-2820 (1993).
- [20] Mercier, A., Mooser, E., Voitchovsky, J.P., “Near edge optical absorption and luminescence of GaSe, GaS and of mixed crystals”, *Journal of Lumin.*, 7: 241-266 (1973).
- [21] Mercier, A., Voitchovsky, J.P., “Donor-acceptor pair recombination and phonon replica in GaS<sub>x</sub>Se<sub>1-x</sub>”, *J. Phys. Chem. Solids*, 36: 1411-1417 (1975).
- [22] Karaman, M.I., Mushinskii, V.P., *Sov. Phys. Semicond.*, 4: 464 (1970).
- [23] Aydinli, A., Gasanly, N.M., Goksen, K., “Donor-acceptor Pair Recombination in Gallium Sulfide”, *J. Appl. Phys.*, 88:7144-7149 (2000).
- [24] Kuhn, A., Bourdan, A., Rigoult, J., Rimsky, A., “Charge-density analysis of GaS”, *Phys. Rev. B*, 25: 4081-4088 (1982).
- [25] Fuchs, M., Scheffler, M., “Ab initio pseudopotentials for electronic structure calculations of poly-atomic systems using density-functional theory”, *Comput. Phys. Commun.*, 119: 67-98 (1999).
- [26] Troullier, N., Martins, J.L., “Efficient pseudopotentials for plane-wave calculations”, *Phys. Rev. B*, 43: 1993-2006 (1990).
- [27] Perdew, J.P., Burke, K., Ernzerhof, M., “Generalized Gradient Approximation Made Simple”, *Phys. Rev. Lett.*, 77: 3865-3868 (1996).
- [28] Perdew, J.P., Wang, Y., “Accurate and simple analytic representation of the electron-gas correlation energy”, *Phys. Rev. B*, 45: 13244-13249 (1992).
- [29] Payne, M.C., Teter, M.P., Allan, D.C., Arias, T.A., Joannopoulos, J.D., “Iterative minimization techniques for ab initio total-energy calculations: molecular dynamics and conjugate gradients”, *Rev. Mod. Phys.*, 64: 1045-1097 (1992).
- [30] Gonze, X., Beuken, J.M., Caracas, R., Detraux, F., Fuchs, M., Rignanese, G.M., Sindic, L., Verstrate, M., Zerah, G., Jollet, F., Torrent, M., Roy, A., Mikami, M., Ghosez, P., Raty, J.Y., Allan, D.C., “First-principle computation of material properties: the ABINIT software project”, *Comput. Mater. Sci.*, 25: 478-492 (2002).
- [31] Kohn, W., Sham, L.J., “Self-Consistent Equations Including Exchange and Correlation Effects”, *Phys. Rev.*, 140: A1133-A1138 (1965).
- [32] Monkhorst, H.J., Pack, J.D., “Special points for Brillouin-zone integrations”, *Phys. Rev. B*, 13: 5188-5192 (1976).
- [33] Akkus, H., Mamedov, A.M., Kazempur, A., Akbarzadeh, H., “Band structure and optical properties of antimony-sulfobromide: density functional calculation”, *Central European Journal of Physics*, 6: 64-75 (2008).
- [34] Hughes, J.L.P., Sipe, J.E., “Calculation of second-order optical response in semiconductors”, *Phys. Rev. B*, 53:10751-10763 (1996).
- [35] Philipp, H.R., Ehrenreich, H., “Optical properties of semiconductors”, *Phys. Rev.*, 129: 1550-1560 (1963).